

---

# MHD flow of viscoelastic nanofluid over a stretching sheet in a porous medium with heat source and chemical reaction

**Kharabela Swain<sup>1,\*</sup>, Sampada Kumar Parida<sup>2</sup>, Gouranga Charan Dash<sup>2</sup>**

1. Department of Mathematics, Radhakrishna Institute of Technology and Engineering, Bhubaneswar 752057, India

2. Department of Mathematics, Siksha 'O' Anusandhan (Deemed to be University), Bhubaneswar 751030, India

kharabela1983@gmail.com

---

*ABSTRACT.* The present study investigates the heat and mass transfer of MHD viscoelastic (Walters' B' model) nanofluid flow over a stretching sheet embedded in a saturated porous medium subject to thermal slip and temperature jump. A simulation model is established through the analysis on relevant constraints such as stretching of bounding surface keeping the origin fixed and thermal slip and temperature jump on the boundary. The numerical solutions are obtained by Runge-Kutta fourth order method with shooting technique. The affects of important thermo-physical parameters on the velocity, temperature, concentration and surface criteria are displayed and analyzed through graphs and tables. As a result of the analysis, the following observations are made. Elasticity of the base fluid in the presence of nanoparticle acts adversely to the growth of velocity as well as thermal boundary layers. Brownian diffusion, thermophoresis and heat source enhance the fluid temperature resulting the cooling of the stretching surface. Further, positive values of heat and mass fluxes for different values of elastic, magnetic and permeability parameters indicate that heat and mass transfer occur from the stretching surface to the fluid. These recommendations are useful to limit the parameters to design viable heat exchangers.

*RÉSUMÉ.* La présente étude examine le transfert de chaleur et de masse du flux de nanofluide viscoélastique MHD (modèle de Walters) sur une feuille d'étirement encastrée dans un milieu poreux saturé soumis au glissement thermique et au saut de température. Un modèle de simulation est établi par l'analyse de contraintes pertinentes, telles que l'étirement de la surface de délimitation en maintenant l'origine, le glissement thermique et le saut de température sur la limite. Les solutions numériques sont obtenues par la méthode de l'ordre quatre de Runge-Kutta avec technique d'injection. Les effets d'importants paramètres thermo-physiques sur les critères de vitesse, de température, de concentration et de surface sont présentés et analysés au moyen de graphiques et de tableaux. À la suite de l'analyse, les observations suivantes sont faites. L'élasticité du fluide de base en présence de nanoparticules agit négativement sur la croissance de la vitesse ainsi que sur les couches limites thermiques.

*La diffusion brownienne, la thermophorèse et la source de chaleur augmentent la température du fluide, ce qui entraîne le refroidissement de la surface d'étirement. En outre, des valeurs positives des flux de chaleur et de masse pour différentes valeurs de paramètres élastiques, magnétiques et de perméabilité indiquent que des transferts de chaleur et de masse ont lieu de la surface d'étirement au fluide. Ces recommandations sont utiles pour limiter les paramètres permettant de concevoir des échangeurs de chaleur viables.*

**KEYWORDS:** MHD, viscoelastic, nanofluid, chemical reaction, heat source/sink.

**MOTS-CLÉS:** MHD, viscoélastique, nanofluide, réaction chimique, source de chaleur/dissipateur.

DOI:10.3166/ACSM.42.7-21 © 2018 Lavoisier

## 1. Introduction

The experiment on thick liquids (condensed milk, liquid lubricant, colloids etc.) showed a considerable deviation from the linear stress-rate of strain relationship. The technological importance of the liquids with elasticity or memory warrants a great importance to study this class of fluids. Crane (1970) and Carragher and Crane (1982) provided a closed form solution for the flow over a stretching a sheet. The MHD flow on boundary layer over a stretching surface has wide applications in chemical, mechanical, industrial and manufacturing processes such as aero dynamics, polymer production, metal casting etc. The flow over a stretching surface moving with continual velocity was studied by Sakiadis (1961). The numerical solution of unsteady MHD flow with heat source and dissipation over a stretching sheet was analyzed by Reddy *et al.*, (2015) and Dessie and Kishan (2014). Rout *et al.*, (2016) have studied the free convective MHD micropolar fluid with chemical reaction.

Nanofluids, combination of base fluid and nanoparticle (1–100 nm), are used to enhance the thermal conductivity of the base fluids such as microelectronics, exchanging devices, melt of polymers, solar collectors, biological solutions, nuclear applications etc. Hayat *et al.*, (2016) studied the MHD flow of non-Newtonian fluid with heat source numerically. Daniel (2015) studied the slip flow mechanism of nanofluid of a stretching sheet. Thermal instability of nanofluid was investigated by Nield and Kuznetsov (2009). Nandy and Pop (2014) and Khan and Pop (2010) have discussed MHD stagnation flow on a shrinking and stretching surface respectively.

Nayak *et al.* (2016) have studied the MHD viscoelastic fluid through porous medium using Walters'  $B'$  fluid model. Popoola *et al.*, (2016) have numerically analyzed the effect of chemical reaction on MHD viscoelastic fluid. Farooq *et al.*, (2016) and Kar *et al.*, (2014) have studied the MHD viscoelastic nanofluid with non-linear thermal radiation. The effect of non-uniform heat source on MHD viscoelastic fluid was studied by Tripathy *et al.*, (2016) and Abel *et al.*, (2007). Buongiorno (2006) observed that for laminar flow, thermophoresis and Brownian diffusion are important mechanisms.

The present analysis considers the solution of nanofluid is an ideal one. The volumes of the components of nanofluid are additive, hence the volume fraction of nanoparticle coincides with concentration. Therefore, separate consideration of

volume fraction has not been taken into account. Despite the above assumption, the present model has following unique features which have not drawn much attention of the researchers. Consideration of viscoelastic fluid (Walters'  $B'$  model) has been considered as the base fluid. The interaction of conducting viscoelastic fluid with an applied transverse magnetic field gives rise to an additional resistive body force has been considered also. The consideration of chemical reaction in the solutal concentration as well as heat source in the heat energy equation enriches the discussion by contributing their effects on flow and heat transfer phenomena. Most importantly, consideration of temperature jump and thermal slip with melting temperature of the surface conditions, embodied in the boundary conditions contribute to mathematical complexity and enliven the possibility of application in the real world problems.

## 2. Mathematical analysis

Consider the two dimensional steady MHD flow of viscoelastic nanofluid in the presence of heat source/sink and chemical reaction on a non-conducting stretching sheet  $y=0$ , embedded in a saturated porous medium with uniform porosity. The flow being is confined to the region  $y>0$ . The velocity, temperature and concentration of the melting stretching sheet are  $u_w(x)=\alpha x$  ( $\alpha>0$ ),  $T_m$  ( $T_m<T_\infty$ ) and  $C_w$  ( $C_w<C_\infty$ ) respectively. The coordinate system describing the flow is given in Fig. 1.

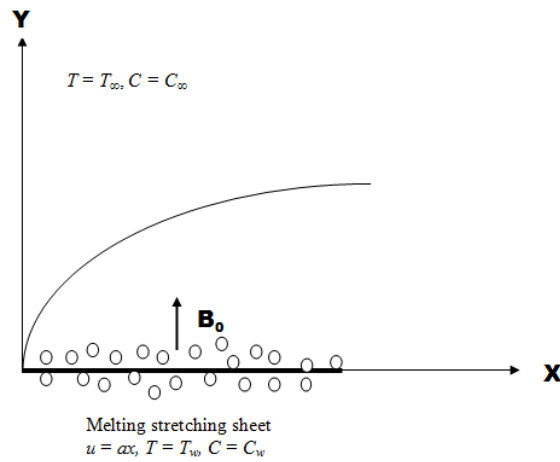


Figure 1. Flow configuration

The governing equations for the nanofluid in Cartesian coordinates following Rashidi *et al.*, (2015) with boundary conditions are given by

$$\frac{\partial u}{\partial x} + \frac{\partial v}{\partial y} = 0 \quad (1)$$

$$u \frac{\partial u}{\partial x} + v \frac{\partial u}{\partial y} = \nu \frac{\partial^2 u}{\partial y^2} - \frac{k_0}{\rho} \left( u \frac{\partial^3 u}{\partial y^2 \partial x} + v \frac{\partial^3 u}{\partial y^3} + \frac{\partial u}{\partial x} \frac{\partial^2 u}{\partial y^2} - \frac{\partial u}{\partial y} \frac{\partial^2 u}{\partial y \partial x} \right) - \frac{\sigma B_0^2}{\rho} u - \frac{\mu}{\rho K p^*} u \quad (2)$$

$$u \frac{\partial T}{\partial x} + v \frac{\partial T}{\partial y} = \alpha \frac{\partial^2 T}{\partial y^2} + \tau \left[ D_B \frac{\partial C}{\partial y} \frac{\partial T}{\partial y} + \frac{D_T}{T_\infty} \left( \frac{\partial T}{\partial y} \right)^2 \right] + \frac{Q_0}{(\rho c_p)_f} (T - T_\infty) \quad (3)$$

$$u \frac{\partial C}{\partial x} + v \frac{\partial C}{\partial y} = D_B \frac{\partial^2 C}{\partial y^2} + \frac{D_T}{T_\infty} \frac{\partial^2 T}{\partial y^2} - k_c (C - C_w) \quad (4)$$

$$\left. \begin{aligned} u = u_w(x) = ax, v = 0, T = T_m, C = C_w \text{ at } y = 0 \\ k \left( \frac{\partial T}{\partial y} \right)_{y=0} = \rho [\beta + c_s (T_m - T_0)] v(x, 0) \\ u = 0, v = 0, T \rightarrow T_\infty, C \rightarrow C_\infty \text{ as } y \rightarrow \infty \end{aligned} \right\} \quad (5)$$

By using the following similarity transformations

$$\psi = (av)^{1/2} x f(\eta), \eta = \left( \frac{\alpha}{\nu} \right)^{1/2} y, \theta(\eta) = \frac{T - T_m}{T_\infty - T_m}, \phi(\eta) = \frac{C - C_w}{C_\infty - C_w} \quad (6)$$

with stream function  $\psi(x,y)$  such that  $u = \partial\psi/\partial y$  and  $v = -\partial\psi/\partial x$ , the equations (2) - (4) and boundary conditions (5) reduce to

$$f''' + ff'' - (f')^2 - Rc \left[ 2ff''' - ff^{IV} - (f'')^2 \right] - (M + Kp) f' = 0 \quad (7)$$

$$\theta'' + Pr \left[ f\theta' + Nb\theta'\phi' + Nt(\theta')^2 + Q\theta \right] = 0 \quad (8)$$

$$\phi'' + Le Pr f\phi' + \frac{Nt}{Nb} \theta'' - \gamma Le Pr \phi = 0 \quad (9)$$

$$\left. \begin{aligned} f'(0) = 1, Pr f(0) + Mp\theta'(0) = 0, \theta(0) = 0, \phi(0) = 0 \\ f'(\infty) = 0, \theta(\infty) = 1, \phi(\infty) = 1 \end{aligned} \right\} \quad (10)$$

where non-dimensional variables and parameters are

$$M = \frac{\sigma B_0^2}{\rho a}, Kp = \frac{Kp^* a}{\nu}, Pr = \frac{\nu}{\alpha}, Le = \frac{\alpha}{D_B}, Rc = \frac{k_0 a}{\nu \rho}, \gamma = \frac{k_c}{a}$$

$$Nb = \frac{\tau D_B (C_\infty - C_w)}{\nu}, Nt = \frac{\tau D_T (T_\infty - T_m)}{\nu T_\infty} \text{ and } Mp = \frac{c_f (T_\infty - T_m)}{\beta + c_s (T_m - T_0)}$$

### 3. Skin friction, heat and mass transfer coefficients

The shearing stress, surface heat flux and surface mass flux are given by

$$\tau_w = \mu \left( \frac{\partial u}{\partial y} \right)_{y=0} - k_0 \left( u \frac{\partial^2 u}{\partial x \partial y} + \nu \frac{\partial^2 u}{\partial y^2} + \frac{\partial u}{\partial x} \frac{\partial u}{\partial y} \right), q_w = -k \left( \frac{\partial T}{\partial y} \right)_{y=0}, q_m = -D_B \left( \frac{\partial C}{\partial y} \right)_{y=0}$$

The non dimensional shear stress coefficient  $C_f = \frac{\tau_w}{\rho U_w^2}$ , local Nusselt number

$Nu_x = \frac{x q_w}{k (T_\infty - T_m)}$ , local Sherwood number  $Sh_x = \frac{x q_m}{D_B (C_\infty - C_w)}$  are given by

$$\left. \begin{aligned} C_f (Re_x)^{1/2} &= (1 - Rc) f''(0) \\ Nu_x (Re_x)^{-1/2} &= -\theta'(0) \\ Sh_x (Re_x)^{-1/2} &= -\phi'(0) \end{aligned} \right\} \quad (11)$$

where  $Re_x = \frac{\alpha x^2}{\nu}$  (local Reynolds number).

From the above, it is seen that the equation (7) is of fourth order. If we consider the viscous liquid only ( $Rc=0$ ), the equation reduces to third order. The two boundary conditions are given explicitly and one implicitly. Therefore, the particular form of the equation admits of a solution as outlined by Abel et al. (2007)

$$f = \frac{1 - e^{-\alpha \eta}}{\alpha} \text{ with } \alpha = \sqrt{\frac{1 + M + Kp}{1 - Rc}} \quad (12)$$

### 4. Method of solution

In the boundary conditions (equation (10)),  $M_p=0$  reduces the problem to no thermal slip and one boundary condition of  $f$  is available (i.e.  $f(0)=0$ ) as such the problem reduces to a third order for  $Rc=0$  and  $M_p=0$  (viscous flow). An approximate analytical solution is possible. In this solution of momentum equation, we have obtained exact solution following Abel *et al.*, (2007). The heat and solutal equations

are solved numerically by reducing the equations to a system of first order equations applying Runge-Kutta fourth order method associated with shooting technique, an iterative procedure for correction of the guess values used as initial conditions with an error tolerance of  $10^{-4}$ . For brevity the details of the solution procedure are not presented here.

## 5. Results and discussion

Though the solution (12) of the momentum equation is in exponential form, and hence asymptotic profiles are expected still then some figures are presented in order to have insight to the effects of the parameters. Figure 2 exhibits the effect of magnetic parameter ( $M$ ) and porosity parameter ( $Kp$ ) on velocity. It is observed that both the parameters have a decelerating effect on the velocity producing a thinner boundary layer. The reason is obvious due to resistive electromagnetic force opposing the flow in the primary or main direction. Similar reason may be attributed to the porosity parameter due to presence of porous matrix which gives rise to the force (body force) acting in the flow domain.

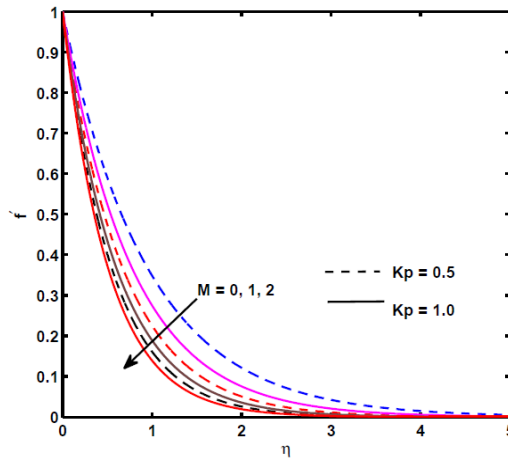


Figure 2. Velocity profiles for various values of  $M$  and  $Kp$  when  $Rc = 0.1$

Figure 3 depicts the same decelerating effect with an increase in viscoelastic parameter. The viscoelastic parameter is a measure of a certain amount of energy which is stored up in the material as strain energy in addition to viscous dissipation. As  $Rc$  increases, the more amount of energy is stored up, hence the velocity reduces. On the other hand in an inelastic viscous liquid we are concerned with the rate of strain but in elastic liquid we cannot neglect strain however small which is responsible for the recovery to the original state and for the reverse flow on removable of stress.

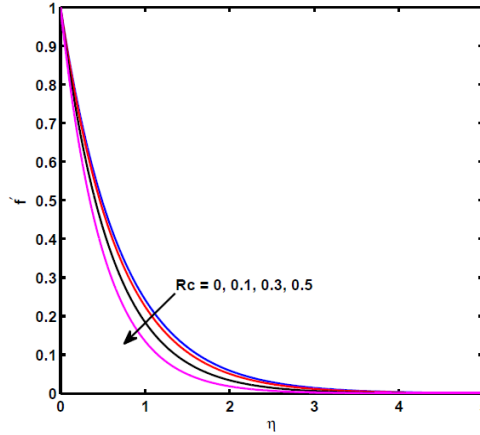


Figure 3. Velocity profiles for various values of  $Rc$  when  $M=Kp=0.5$

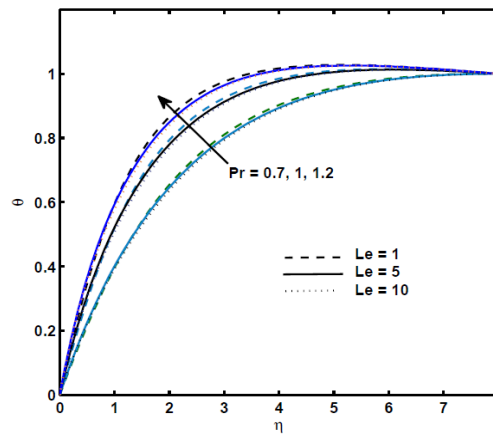


Figure 4. Temperature profiles for various values of  $Le$  and  $Pr$  when  $M=1.0$ ,  $Kp=0.5$ ,  $Q=0.01$ ,  $Nb=0.5$ ,  $Nt=0.1$ ,  $\gamma=0.01$ ,  $Rc=0.1$

Figures 4, 5 and 6 exhibit the temperature distribution in the thermal boundary layer. It is seen that  $Pr$ ,  $Nt$ ,  $Nb$  and  $Q$  enhance the temperature at all points of the flow domain whereas  $Rc$  and  $Le$  decrease the temperature slightly. The decrease in temperature due to increase in elastic parameter (due to higher stored up energy) as explained earlier. The Lewis number  $Le$  is the ratio of thermal diffusivity of base fluid and Brownian diffusion coefficient of nanoparticle. This is an important parameter in nanofluid flow analogous to Reynolds number, Prandtl number, and Schmidt number. The physical parameters  $Re$ ,  $Pr$  and  $Sc$  exhibit relative measure of momentum

diffusivity with viscosity, momentum diffusivity with thermal diffusivity and momentum diffusivity with mass diffusivity. Figure 4 shows that  $Le$  have no significant effect on temperature distribution. To sum up, both elasticity parameter and Lewis number have no significant effect on the temperature distribution. Higher Prandtl number fluid (Figure 4) and heat source (Figure 6) gives rise to higher temperature. As regard to Brownian motion parameter ( $Nb$ ) and thermophoresis parameter ( $Nt$ ), it is pointed out that the coincidence of profiles for  $Nb=0.1$ , and  $Nb=0.3$  (Figure 5) asserts that Brownian motion has no significant effect on temperature field. On the other hand  $Nt$ , contributes to rise in temperature.

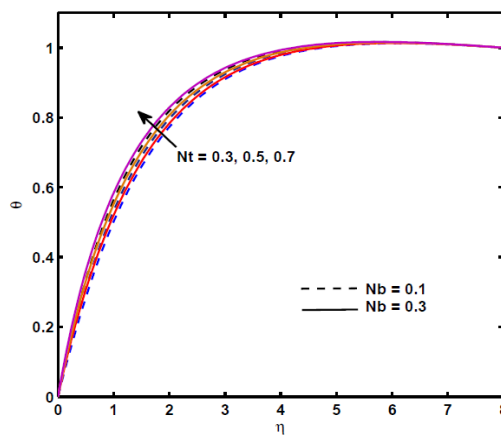


Figure 5. Temperature profiles for various values of  $Nb$  and  $Nt$  when  $M=1.0$ ,  $Kp=0.5$ ,  $Q=0.01$ ,  $Le=10.0$ ,  $Pr=1.0$ ,  $\gamma=0.01$ ,  $Rc=0.1$

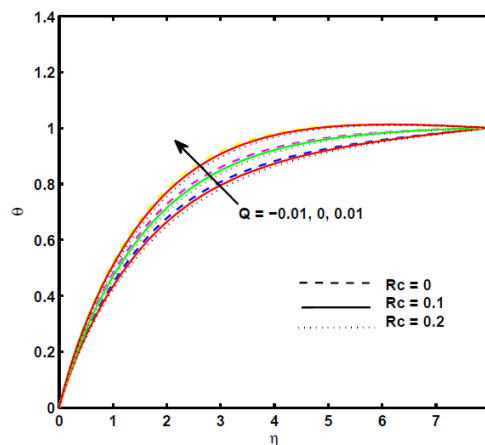


Figure 6. Temperature profiles for various values of  $Q$  and  $Rc$  when  $M=1.0$ ,  $Kp=0.5$ ,  $Le=10$ ,  $Nb=0.5$ ,  $Nt=0.1$ ,  $\gamma=0.01$ ,  $Pr=1.0$

Figure 7 displays the solutal concentration due to nanoparticle diffusion to base fluid. The Lewis number modifies the concentration (volume fraction) distribution significantly in conjunction with higher Prandtl number fluid. The rise in concentration level is quite significant when  $Le$  increases from 1 to 5 (i.e. under the dominating effect of Brownian diffusivity over thermal diffusivity). The rise is significant within the layers close to stretching surface then the effect subsides. The reason may be attributed as under: layers close to the stretching surface have a shearing effect and far off layers have a little, representing potential flow. Hence, it is concluded that Brownian diffusion enhances the solutal boundary layer thickness significantly. On careful study it reveals that increasing  $Le$  from 5 to 10 does not contribute much as compared to that of  $Le = 1$  and  $Le = 5$ . Thus, the analysis reveals that when thermal diffusivity and Brownian diffusivity are of comparable magnitude i.e.  $Le = 1$ ,  $Pr$  enhances the concentration moderately but in case of higher Prandtl number base fluid with nanoparticle having dominating diffusivity enhances concentration significantly. This may be taken as a recommendation for the choice of high Prandtl number base fluid and nanoparticle with low thermal diffusivity for achieving adequate mass diffusion to more number of layers enhancing concentration level.

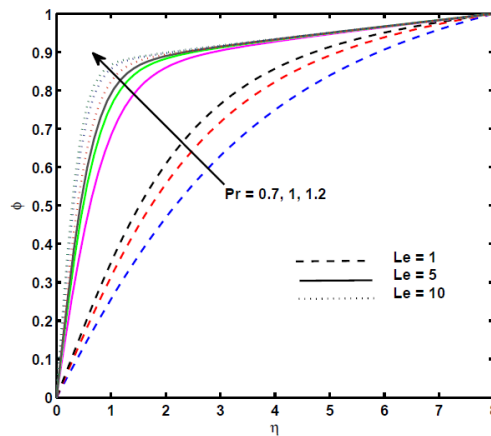


Figure 7. Concentration profiles for various values of  $Le$  and  $Pr$  when  $M=1.0$ ,  $Kp=0.5$ ,  $Q=0.01$ ,  $Nb=0.5$ ,  $Nt=0.1$ ,  $\gamma=0.01$ ,  $Rc=0.1$

The close observation of Figures 8 and 9 exhibit the effects of  $Nt$  (thermophoresis parameter),  $Nb$  (Brownian motion parameter) and  $\gamma$  (chemical reaction parameter) on solutal concentration. The thermophoresis and Brownian motion both constitute two important processes of nanofluid flow. It is interesting to note that Brownian motion favours the growth of concentration level whereas thermophoresis reduces it. The reason may be attributed to enhancing the concentration by the Brownian diffusion  $\left[ Nb = \frac{\tau_D B (C_\infty - C_w)}{\nu}, C_\infty > C_w \right]$  is that as the ambient state remains in the higher concentration level, the mass concentration flows from ambient layers to solutal

boundary layer being assisted by Brownian diffusion and hence, concentration level increases whereas in case of  $Nt$ , the rise of temperature diffuses the mass, reducing the level of concentration. Thus, it is suggested that the ambient temperature and concentration may be adjusted suitably with surface temperature and concentration to obtain the desired result as per the requirement. Further, it is seen from Figure 9 that the level of concentration always decreases with the higher strength of chemical reactions for  $\gamma > 0$  and  $\gamma < 0$  i.e. for both destructive and constructive reactions.

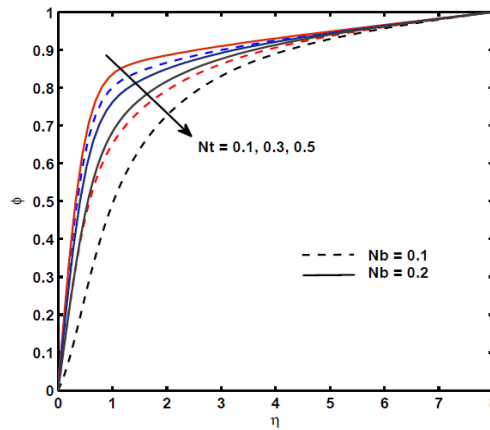


Figure 8. Concentration profiles for various values of  $Nb$  and  $Nt$  when  $M=1.0$ ,  $Kp=0.5$ ,  $Q=0.01$ ,  $Le=10.0$ ,  $Pr=1.0$ ,  $\gamma=0.01$ ,  $Rc=0.1$

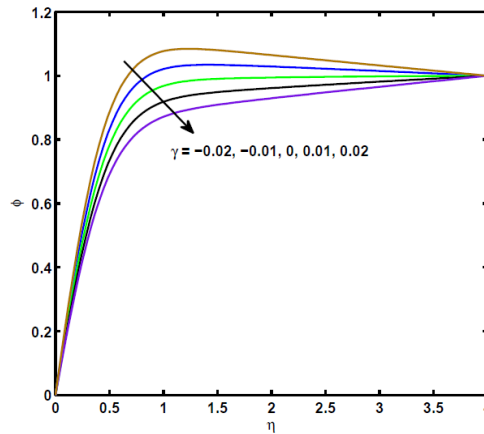


Figure 9. Concentration profiles for various values of  $\gamma$  when  $M=1.0$ ,  $Kp=0.5$ ,  $Q=0.01$ ,  $Le=10.0$ ,  $Pr=1.0$ ,  $Nb=0.5$ ,  $Nt=0.1$ ,  $Rc=0.1$

Table 1. Comparison of shearing stress at the plate

| $Rc$  | Rajagopal et al. (1987) | Present study |
|-------|-------------------------|---------------|
| 0.005 | -0.9975                 | -0.997496     |
| 0.01  | -0.9949                 | -0.994987     |
| 0.03  | -0.9846                 | -0.984885     |
| 0.05  | -0.9738                 | -0.974679     |

Table 2. Wall temperature gradients  $\{-\theta'(0)\}$  and wall nanoparticle volume fraction gradients  $\{-\phi'(0)\}$  for  $Mp=Nb=0.5, Pr=1, Le=5, Nt=0.1, Q=0.01$

| $M$ | $Kp$ | $Rc$ | $-\theta'(0)$ | $-\phi'(0)$ |
|-----|------|------|---------------|-------------|
| 0.5 | 0.5  | 0.1  | 0.786070      | 1.214560    |
| 1   |      |      | 0.744212      | 1.168901    |
| 2   |      |      | 0.679579      | 1.092687    |
|     | 1    |      | 0.653956      | 1.060048    |
|     | 2    |      | 0.611828      | 1.002693    |
|     |      | 0.2  | 0.590141      | 0.971127    |
|     |      | 0.3  | 0.566162      | 0.934406    |

Table 3. Wall temperature gradients  $\{-\theta'(0)\}$  and wall nanoparticle volume fraction gradients  $\{-\phi'(0)\}$  for  $M=Kp=Mp=0.5, Rc=0.1$

| $Pr$ | $Le$ | $Nb$ | $Nt$ | $Q$  | $\gamma$ | $\theta'(0)$ | $\phi'(0)$ |
|------|------|------|------|------|----------|--------------|------------|
| 5    | 1    | 0.5  | 0.1  | 0.1  | 0.1      | 10.393079    | 1.065931   |
| 7    |      |      |      |      |          | 17.154686    | 2.120061   |
|      | 2    |      |      |      |          | 22.470088    | 2.623426   |
|      |      | 1    |      |      |          | 28.525522    | 1.504031   |
|      |      |      | 0.2  |      |          | 47.374062    | 7.354294   |
|      |      |      |      | 0    |          | 8.135904     | 0.469988   |
|      |      |      |      | -0.1 |          | 2.385925     | 0.448819   |
|      |      |      |      |      | 0        | 6.549223     | 1.506576   |
|      |      |      |      |      | -0.1     | 10.295772    | 7.348726   |

Table-1 represents a comparison of shearing stress at the plate with Rajagopal (1987) under restricted conditions when  $M=Kp=0$ . This shows a good agreement. Tables-2 and 3 show that both heat flux and mass flux at the plate are positive for different values of  $M, Kp$ , and  $Rc$ . Thus, it is concluded that heat and mass flow from the stretching surface to the fluid. Further, it is revealed that an increase in magnetic parameter, porosity parameter and viscoelastic parameter enhance both heat and mass fluxes at the plate. The present analysis provides a suggestive measure for cooling the plate. From table-3 it is seen that an increase in  $Pr, Le, Nb$  and  $Nt$ , increase both surface heat flux and mass flux except chemical reaction parameter  $\gamma(\gamma < 0)$  i.e. for constructive reaction or generating reaction. The reason is obvious due to generation

of heat in the fluid, so that the heat and mass flux at the surface increase as the heat and mass diffusion get accelerated.

## 6. Conclusion

- (i) Both elasticity of the fluid and porosity of the medium have decelerating effect on velocity profiles producing thinner boundary layer.
- (ii) Brownian diffusion, thermophoresis and heat source enhance the temperature distribution whereas elasticity and Lewis number decelerate. The close analysis reveals that Brownian diffusivity fails to contribute significantly to the temperature distribution.
- (iii) Lewis number modifies the solutal concentration significantly in conjunction with higher Prandtl number fluid.
- (iv) Brownian diffusivity enhances the concentration whereas thermophoresis decelerates it. The explanation is embodied in the text (Figures. 8 & 9).
- (v) Chemical reaction parameter decelerates the level of concentration in both destructive and generative reactions.
- (vi) Higher magnetic field, elasticity and permeability of the medium contribute to heat and mass transfer from the plate to the fluid, enhancing the thermal energy and solutal concentration level of the nanofluid. Consequently, those parameters contribute to cooling of the plate and other parameters act adversely. Thus, cooling/heating mechanism can be developed by right choice of the fluid model and regulating the governing parameters.

## References

- Abel S., Siddheshwar P. G., Nandeppanavar M. (2007). Heat transfer in a viscoelastic boundary layer flow over a stretching sheet with viscous dissipation and non-uniform heat source. *International Journal of Heat and Mass Transfer*, Vol. 50, pp. 960-966. <http://dx.doi.org/10.1016/j.ijheatmasstransfer.2006.08.010>
- Buongiorno J. (2006). Convective transport in nanofluids. *J. Heat Transfer ASME*, Vol. 128, No. 3, pp. 240-250. <http://dx.doi.org/10.1115/1.2150834>
- Carragher P., Crane L. J. (1982). Heat transfer on a continuous stretching sheet. *Zeit ANGEW Math. Phys*, Vol. 62, pp. 564-565. <http://dx.doi.org/10.1002/zamm.19820621009>
- Crane L. J. (1970). Flow past a stretching plate. *Zeit ANGEW Math. Phys*, Vol. 21, pp. 645-647. <http://dx.doi.org/10.1007/BF01587695>
- Daniel Y. S. (2015). Presence of heat generation/absorption on boundary layer slip flow of nanofluid over a porous stretching sheet. *American Journal of Heat and Mass Transfer*, Vol. 2, No. 1, pp. 15-30. <http://dx.doi.org/10.7726/ajhmt.2015.1002>
- Dessie H., Kishan N. (2014). MHD effects on heat transfer over stretching sheet embedded in porous medium with variable viscosity, viscous dissipation and heat source/sink. *Ain Shams Engineering Journal*, Vol. 5, pp. 967-977. <http://dx.doi.org/10.1016/j.asej.2014.03.008>

- Farooq M., Khan M. I., Waqas M., Hayat T., Khan M. I. (2016). MHD stagnation point flow of viscoelastic nanofluid with non-linear radiation effects. *Journal of Molecular Liquids*, Vol. 221, pp. 1097-1103. <http://dx.doi.org/10.1016/j.molliq.2016.06.077>
- Hayat T., Awais M., Imtiaz A. (2016). Heat source/sink in a magneto-hydrodynamic non-newtonian fluid flow in a porous medium: Dual solutions. *PLoS One*, Vol. 11, No. 9, pp. e0162205. <http://dx.doi.org/10.1371/journal.pone.0162205>
- Kar M., Sahoo S. N., Rath P. K., Dash G. C. (2014). Heat and mass transfer effects on a dissipative and radiative visco-elastic MHD flow over a stretching porous sheet. *Arabian Journal for Science and Engineering*, Vol. 39, No. 5, pp. 3393-3401. <http://dx.doi.org/10.1007/s13369-014-0991-0>
- Khan W. A., Pop I. (2010). Boundary layer flow of a nanofluid past a stretching sheet. *Int. J. Heat and Mass Transfer*, Vol. 53, pp. 2477-2483. <http://dx.doi.org/10.1016/j.ijheatmasstransfer.2010.01.032>
- Nandy S. K., Pop I. (2014). Effects of magnetic field and thermal radiation on stagnation flow and heat transfer of nanofluid over a shrinking surface. *International Communications in Heat and Mass Transfer*, Vol. 53, pp. 50-55. <http://dx.doi.org/10.1016/j.icheatmasstransfer.2014.02.010>
- Nayak M. K., Dash G. C., Singh L. P. (2016). Heat and mass transfer effects on MHD viscoelastic fluid over a stretching sheet through porous medium in presence of chemical reaction. *Propulsion and Power Research*, Vol. 5, No. 1, pp. 70-80. <http://dx.doi.org/10.1016/j.jprr.2016.01.006>
- Nield D. A., Kuznetsov A. V. (2009). Thermal instability in a porous medium layer saturated by a nanofluid. *International Journal of Heat and Mass Transfer*, Vol. 52, pp. 5796-5801. <http://dx.doi.org/10.1016/j.ijheatmasstransfer.2009.07.023>
- Popoola A., Ismail G. B., Olajuwon B. (2016). Heat and mass transfer on MHD Viscoelastic fluid flow in the presence of thermal diffusion and chemical reaction. *International Journal of Heat and Technology*, Vol. 34, No. 1, pp. 15-26. <http://dx.doi.org/10.18280/ijht.340103>
- Rajagopal K. R., Na T. Y., Gupta A. S. (1987). A non similar boundary layer on a stretching sheet in a non-Newtonian fluid with uniform free stream. *J. Math. Phys. Sci.*, Vol. 21, No. 2, pp. 189-200.
- Rashidi M. M., Ali M., Rostami B., Rostami P., Xie G. (2015). Heat and mass transfer for MHD viscoelastic fluid flow over a vertical stretching sheet with considering Soret and Dufour effects. *Mathematical Problems in Engineering*, Vol. 2015, Article ID 861065. <http://dx.doi.org/10.1155/2015/861065>
- Reddy M. G., Padma P., Shankar B. (2015). Effects of viscous dissipation and heat source on unsteady MHD flow over a stretching sheet. *Ain Shams Engineering Journal*, Vol. 6, pp. 1195-1201.
- Rout P. K., Sahoo S. N., Dash G. C., Mishra S. R. (2016). Chemical reaction effect on MHD free convection flow in a micropolar fluid. *Alexandria Engineering Journal*, Vol. 55, pp. 2967-2973. <http://dx.doi.org/10.1016/j.aej.2016.04.033>
- Sakiadis B. C. (1961). Boundary layer behaviours on continuous solid surface. *AIChE J*, Vol. 7, No. 2, pp. 221-5.
- Tripathy R., Mishra S. R., Dash G. C. (2016). Numerical analysis of hydromagnetic micropolar fluid along a stretching sheet embedded in porous medium with non-uniform heat source

and chemical reaction. *Engineering Science and Technology, an International Journal*, Vol. 19, No. 3, pp. 1573-1581. <http://dx.doi.org/10.1016/j.jestch.2016.05.012>

### Nomenclature

|              |  |
|--------------|--|
| $u, v$       | velocity components along the $x$ and $y$ axes |
| $D_B$        | Brownian diffusion coefficient                 |
| $D_T$        | thermophoresis diffusion coefficient           |
| $T$          | nanofluid temperature                          |
| $(\rho c)_f$ | heat capacity of the nanofluid                 |
| $(\rho c)_p$ | effective heat capacity of nanoparticle        |
| $B_0$        | magnetic field strength                        |
| $Kp^*$       | permeability of the porous medium              |
| $k_c$        | chemical reaction coefficient                  |
| $k_0$        | viscoelastic parameter ( $k_0 > 0$ )           |
| $C$          | volumetric volume fraction                     |
| $T_w$        | temperature of the nanofluid near wall         |
| $T_\infty$   | free stream temperature of the nanofluid       |
| $k$          | thermal conductivity                           |
| $c_s$        | heat capacity of the solid surface             |
| $u_w$        | stretching sheet velocity                      |
| $a$          | stretching rate being a positive constant      |
| $b$          | positive constant                              |
| $M$          | magnetic parameter                             |
| $Kp$         | permeability parameter                         |
| $Mp$         | dimensionless melting parameter                |
| $Pr$         | Prandtl number                                 |

|      |                           |
|------|---------------------------|
| $Nb$ | Brownian motion parameter |
| $Nt$ | thermophoresis parameter  |
| $Le$ | Lewis number              |

**Greek symbols**

|            |  |
|------------|--|
| $\eta$     | similarity variable  |
| $\theta$   | dimensionless temperature  |
| $\phi$     | dimensionless concentration  |
| $\rho$     | density of the nanofluid   |
| $\alpha_m$ | nanofluid thermal diffusivity  |
| $\nu$      | kinematic viscosity  |
| $\tau$     | ratio between the effective heat capacity of the nanoparticle material and the fluid |
| $\beta$    | latent heat of the fluid   |
| $\lambda$  | ratio of free stream velocity to stretching sheet                                    |
| $\gamma$   | chemical reaction parameter  |

